Large-Scale Turbulence Effects Simulations for Piston Phase Retrieval

Artem M. Vorontsov[1,3] , Mikhail A. Vorontsov[2,3], and V.S. Rao Gudimetla[4]

1. Moscow State University, Department of Physics, Vorob'evi Gory, Moscow, Russia
2. University of Dayton, School of Engineering, 300 College Park Center, Dayton, OH, 45469-2951
3. Optonicus LLC, 711 E. Monument Ave. Suite 101, Dayton, OH 45402
4. U. S. Air Force Research Laboratory, Directed Energy Directorate, Det. 15, 535 Lipoa Parkway, Kehie, Hi 96753

ABSTRACT

In the conventional atmospheric turbulence numerical simulation techniques based on the "split"-operator method, the turbulence-induced refractive index inhomogeneities are represented by a set of infinitely narrow (2D) phase distorting layers (phase screens). These conventional phase screens cannot represent large-scale refractive index inhomogeneities due to limitations imposed by computational grid size. For this reason, this commonly used model cannot be applied for computer analysis of atmospheric optical systems that are affected by the presence of large-scale turbulence eddies. Among these systems are coherent imaging ladars, optical vibrometers and interferometers. In the classical Kolmogorov turbulence theory, the impact of the large-scale turbulence eddies are associated with the turbulence outer scale. Contrary to the conventional approach, in the computer simulation technique introduced here the turbulence-induced refractive index inhomogeneities are represented by a set of large-scale phase distorting screens that account for refractive index inhomogeneities which extend beyond the numerical grid correlation length. The results are applied to the analysis of piston phase fluctuations for the cases when the turbulence outer scale significantly exceeds the receiver aperture size. We also analyze the piston phase fluctuations in deep turbulence conditions in presence of phase singularities (phase cuts and branch points), and show that the conventional definition of piston phase cannot be applied for this case. We introduce a more general definition of piston phase which is useful for analysis in deep turbulence conditions.

1. INTRODUCTION

The efficiency of various optical systems based on coherent detection techniques heavily depends on the accurate prediction of statistical and temporal characteristics of the aperture averaged (piston) phase [1]. The rigorous estimation of the piston phase represents a quite challenging task, since the piston phase depends strongly on large-scale turbulent eddies with sizes on the order of or exceeding the receive aperture diameter D [2]. Although the smaller size turbulent eddies can also affect piston phase values, their impact is less profound due to aperture averaging. Thus, accurate estimation of piston phase cannot be performed without consideration of the largest size refractive index fluctuations. Within the framework of the fully-developed Kolmogorov turbulence model, the largest scale eddies are described by the turbulence outer scale L_0, whose size, ranging from a few to hundreds of meters, can significantly exceed the receiver aperture diameter D.

Predictive modeling of optical wave propagation and piston phase estimation is currently performed using the conventional representation of Kolmogorov's turbulence by a set of *statistically independent, infinitely thin two-dimensional* phase screens, which are *spatially bounded* inside a numerical grid domain. This conventional approach creates significant problems in the analysis of optical systems (including coherent detection systems) whose performance depends on large-scale turbulent eddies. In the conventional numerical simulation techniques used for phase screen generation, the turbulence outer scale L_0 is associated with the numerical grid size and exceeds D only by a few fold (typically from four to eight fold only). Because of practical considerations related to acceptable duration of the computation time and available computer memory, in most predictive wave-optics simulations the grid size typically doesn't exceed 1024×1024 (more commonly 512×512) and accordingly, the corresponding analysis is limited by atmospheric conditions for which the outer scale L_0 is on the order of the receiver aperture diameter D. Clearly, piston phase estimations based on wave optics simulations that utilize such conventional phase screen generation techniques, may not fully account for the impact of large-scale turbulent eddies and this may lead to significant errors.

Another serious problem arises in modeling of the temporal dynamics of the piston phase in tracking of moving objects. In this application, wave propagation occurs under conditions of continuously changing optical axis direction and potential crossing of several atmospheric layers, which may have different turbulence properties over

the propagation path. All these propagation scenarios require consideration of a large region of the atmosphere, which may need significantly large almost impractical numerical grid size. In this paper we address these problems by applying for piston phase analysis the recently developed infinitively long phase screen (ILPS) technique [3]. In the following section we briefly describe the ILPS technique. Analysis of piston phase fluctuation variance is presented in section 3.

2. GENERATION OF PHASE SCREENS WITH ARBITRARY LARGE TURBULENCE OUTER SCALE

In the conventional phase screen generation technique, a random function $S = S(m,n)$, defined inside a square grid, is computed using Fourier transform of the product of refractive index fluctuation power spectrum function $\Phi(k,l)$ and the delta-correlated on the $N \times N$ grid complex random function $\eta(k,l)$ with uniform probability distribution inside [0, 1] interval, as:

\

$$S(m,n) = FT\left[\sqrt{\Phi(k,l)}\eta(k,l)\right](m,n), \tag{1}$$

where (m,n), $m,n \in \{1,...,N\}$ and (k,l), $k,l \in \{1,...,N\}$) are integer numbers corresponding to numerical grid pixels and FT is the Fourier transform operator. For statistically independent real and imaginary components of function $\eta(k,l)$ the complex function S is comprised of two statistically independent (component) phase screens. These functions are periodic with the numerical grid size period. The examples of the conventional phase screens are shown in Fig. 1.

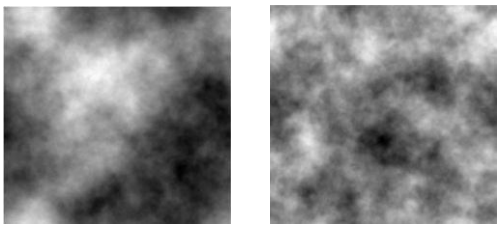

Fig. 1. Grey scale representation of the generated on 512×512 grid random phase screen realizations with different power spectrums: Kolmogorov (left) and Tatarskii (right).

In the next step, consider computer generation of a phase screen S that is defined inside an extended in one direction grid of size $JN \times N$, where J is the grid extension factor ($J = 2,3,...$). As shown in [4] such phase screen can be obtained by summarizing J conventional random phase screen functions $S_j(m,n)$ ($j \in \{1,...,J\}$) as defined by expression (1) with exponential weighting factors:

$$S(m,n) = \sum_{j=1}^{J} e^{i\frac{2\pi jm}{JN}} S_j(m,n), \tag{2}$$

where $m \in \{1,..,JN\}$ and $n \in \{1,..,N\}$, and $i^2 = -1$. Note that the obtained new phase screen S is a periodic function with the period JN along x and N along y directions. In the coordinate space, the extended grid corresponds to $L_x L_y$ area, where $L_x = dxJN$ and $L_y = dyN$ and dx and dy are pixel lengths in physics units. Examples of phase screens obtained on an extended grid (extended phase screens) are shown in Fig. 2.

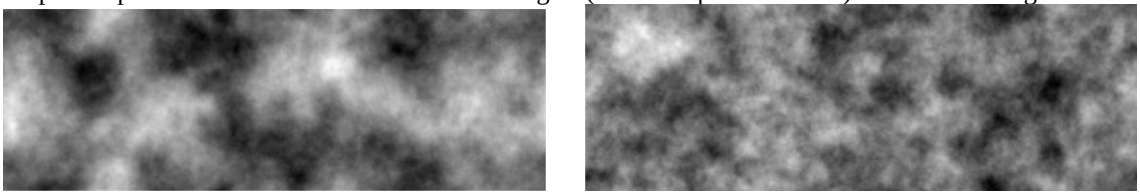

Fig. 2. Gray scale representation of the generated extended phase screens corresponding to Kolmogorov (top) and Tatarskii (bottom) power spectra on the numerical grid containing 4*512×512 pixels (the grid extension factor *J*=4).

Generation of phase screens with arbitrary large turbulence outer scale L_0 can now be performed by utilizing the extended phase screen technique described above. The idea is based on partitioning of the spectral domain of the refractive index power spectrum function Φ with a predefined outer scale value L_0 onto $H > 1$ (H is an integer number) spectral sub-regions and generation of the extended phase screens $S_h(\mathbf{r})$, where $h \in \{1,...,H\}$, with the power spectrum functions $\Phi_h(\boldsymbol{\kappa})$ that coincide with Φ inside these sub-regions and equal to zero otherwise. Here $\boldsymbol{\kappa}$ is a vector in the spectral domain. Consider as an example partitioning of the spectral domain onto sub-regions in the form of concentric annuli $\{K_h\}_{h=1}^{H}$ centered at the coordinate origin. As shown in [3], phase screens corresponding to the power spectrum Φ with outer scale L_0 can be obtained using summation of the extended phase screens $S_h(\mathbf{r})$ corresponding to the power spectrum functions $\Phi_h(\boldsymbol{\kappa})$:

$$S(\mathbf{r}) = \sum_{h=1}^{H} S_h(\mathbf{r}) \tag{3}$$

The extended phase screens $S_h(\mathbf{r})$ are defined inside coordinate domain $L_x = dxJN > L_0$, $L_y = dyN$ and are generated using the described above technique. An example of phase screen with Tatarskii power spectrum and $L_0 = 7L_y$ is presented in Fig. 3. Note that fusion of the extended phase screens $S_h(\mathbf{r})$ that are generated inside coordinate domains with different pixel sizes dx_h and dy_h, requires additional computation (approximation and filtering) to unify grid pixel sizes prior to the fusion [3].

Fig. 3. Gray scale representation of phase screen corresponding to Tatarskii power spectrum with the outer scale L_0 that is seven fold longer than the phase screen width. The phase screen is generated using numerical grid with 8*512×512 (J=8) pixels.

In any numerical simulations of atmospheric optical systems, temporal dynamics of the atmospheric turbulence may play an important role. Conventional approach to include turbulence induced temporal variations in system performance is based on Taylor's hypothesis of "frozen" refractive index inhomogeneities that are moved as a whole with a wind velocity $\mathbf{v}$. In the split operator technique described, the wind induced temporal variations inside optical system aperture are simulated by introducing a set lateral shifts of phase screens over distance dx, that corresponds to the grid pixel size in the direction orthogonal to the system optical. The characteristic time T_G for the complete update of the extended phase screen realization that is defined inside coordinate domain $L_x = dxJN > L_0$, $L_y = dyN$ equals to $T_G = L_x / v_x < L_0 / v_x$, where v_x is x- projection of wind velocity vector $\mathbf{v}$. For simplicity we assume that $v_y = 0$. Thus the conventional approach of phase screens generation allows only analysis of temporal dynamics over time $T < T_G$ that is associated with impact of a single turbulence eddy of size L_0. This restriction significantly limits ability to compute time-averaged characteristics that are dependent on the turbulence outer scale, such as piston phase, and hence require computer simulation of temporal dynamics over the time $T < T_G$ that significantly exceeds the time of the extended phase screen update time. As shown in [3], this problem can be resolved by applying the infinitively-long (IL) phase screen technique.

Assume a set of the extended phase screens $S_j^{IL} = S_j^{IL}(m,n)$, where $j \in \{1,...,J_{IL}\}$. Here $J_{IL} = pJ$ and $p \geq 2$ is an integer. Each of these extended phase screens are generated using the described above technique and are defined inside the extended grid with $JN \times N$ pixels. Consider the following defining the infinitely long phase screen expression

$$S^{IL}(m,n)=\sum_{j=0}^{J_{IL}}\psi_j(m,n)\,S_j^{IL}(m-jM,n), \tag{4}$$

where $\psi_j(m,n)=\cos(\pi m/J_{IL}N)$, $M=J_{IL}N/2$, $m>1$ and $n\in\{1,...,N\}$. Note that the $S^{IL}=S^{IL}(m,n)$ is defined inside an infinite in x-direction grid. As shown in [4], the random function S^{IL} defined by (4) has approximately identical statistical properties as random functions $\{S_j^{IL}\}_{j=1}^{J_{IL}}$. Note that in each grid point (m,n) function $S_j^{IL}(m,n)$ is composed of only two statistically independent extended phase screen functions multiplied by the weighting factors $\psi_j(m,n)$ and $\psi_{j+1}(m,n)$: random function realization S_j^{IL} and the shifted over M pixels in x-direction random function S_{j+1}^{IL} as illustrated in Fig. 4. This means that for computer simulation of temporal dynamics over an arbitrary long time $T>T_G$ using sequential shifts of phase screens, there is no need for generation and keeping in the computer memory of large number J_{IL} of random functions S_j^{IL}, ($j\in\{1,...,J_{IL}\}$). In fact, the same goal can be achieved by generation and saving in computer memory only two extended phase screens (S_j^{IL} and S_{j+1}^{IL}). The weighted combination of these functions S_j^{IL} as described by (4) can be used until the lateral shift of the phase screen S_j^{IL} approaches the extended grid boundary. At this point an additional the extended phase screen S_{j+2}^{IL} should be generated. The temporal dynamics inside the next time interval of duration T_G is now defines by phase screen S^{IL} that contains weighted combination of functions S_{j+1}^{IL} and S_{j+2}^{IL}. This process of regeneration of extended phase screens and their fusion can be repeated as many times as required for analyzing an optical system dynamics over arbitrary long time.

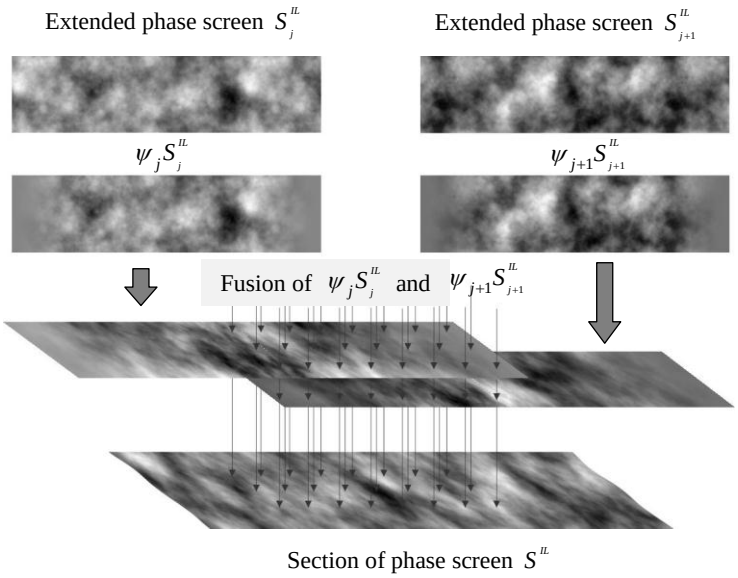

Fig. 4. Graphical illustration of an infinitely long phase screen generation technique.

3. STATISTICAL CHARACTERISTICS OF PISTON PHASE: NUMERICAL SIMULATION RESULTS

3.1 <u>Pupil-plane phase screen model.</u> In this section we consider statistical characteristics of piston phase measured at a receiver telescope of diameter *D* which are obtained through numerical simulation of plane wave propagation through a moving with wind velocity $\mathbf{v}=(v_x,0)$ atmospheric turbulence. The commonly used definition of piston phase is given by the following expression:

$$\overline{\varphi}(t) = \frac{1}{S_a}\int_{s_a} \varphi(\mathbf{r},t)\, d^2\mathbf{r} \tag{5}$$

where $\varphi(\mathbf{r},t)$ is the instantaneous phase function defined inside the receiver telescope aperture area S_a. First assume that the impact of atmospheric turbulence can be described by a single thin phase screen that is located at the telescope pupil (pupil-plane phase screens). This model is commonly used for analysis of optical propagation in the Earth atmosphere at high elevation angles. In the numerical simulations of piston phase dynamics, we used pupil-plane phase screens with Tatarskii refractive index fluctuation power spectrum with a fixed parameter C_n^2 and different values of the turbulence outer scales L_0 ranging from $L_0 = D$ to $L_0 = 10D$. The numerical simulations were performed for receiver aperture of diameters D=3.6 m and D=1.0 m. We also assumed that all temporal changes in the piston phase are due to lateral translation of the phase screen with a constant wind speed $\mathbf{v}=(v_x=1.0$ m/sec, $0)$. In the numerical generation of phase screens the grid extension factor J in (2) was varied depending on the chosen value of the outer scale value L_0. We simulated piston phase dynamics in T =24 min time intervals. This time interval corresponds to translation through the receiver aperture D of the pupil plane turbulent screen of length $400D$. The total length of effective phase screen was controlled by setting parameter J_{IL} in (4).

Examples of piston phase dynamics for two different values of the outer scale are presented in Fig. 5. The results suggest that increase of L_0 leads to rapid increase of piston phase fluctuations. Using the piston phase temporal evolution curves as in Fig. 5, we estimated the standard deviation of piston phase fluctuations $\sigma = \left\langle \left[\overline{\varphi}(t) - \left\langle \overline{\varphi}(t) \right\rangle \right]^2 \right\rangle^{1/2}$. In computation of σ, we substituted ensemble averaging by time averaging over 24 min observation time. The results of σ estimation are shown in Fig. 6 for two different receiver aperture diameters. The standard deviation of piston phase fluctuations rapidly increases with the outer scale increase reaching 2π value at $L_0 \approx 36$m in the example considered. At the same time σ only weakly depends on the receiver aperture size (compare two curves corresponding to D=3.6 m and D=1.0 m in Fig. 6).

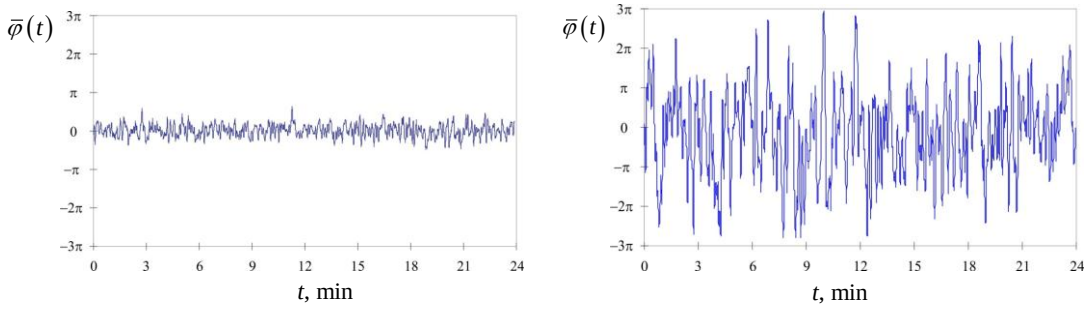

Fig. 5. Temporal evolution of piston phase for $L_0 = D$ (left) and $L_0 = 5D$ (right) for $C_n^2 = 10^{-15}$ m$^{-2/}$3, and D=3.6 m.

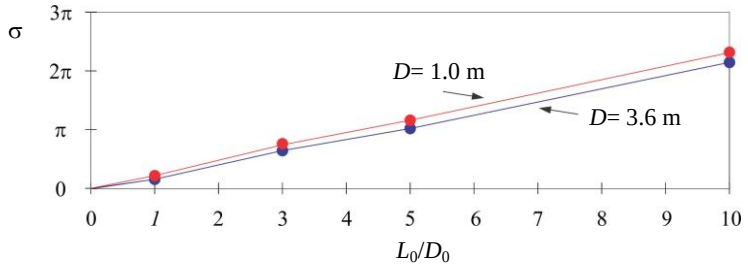

Fig. 6. Piston phase standard deviation σ vs turbulence outer scale L_0 for $C_n^2 = 10^{-15}$ m$^{-2/}$3 .

Consider now the dynamics of piston phase for slant propagation paths. In these propagation scenarios, phase function $\varphi(\mathbf{r},t)$ of entering receiver aperture optical field is characterized by the presence of intensity scintillations, 2π–phase cuts and branch points. The first question to ask is how to define piston phase for slant propagation

conditions by taking into account sensitivity of piston phase value to geometry of 2π–phase cuts and branch points. Indeed in presence of these phase singularities, the commonly used definition of piston phase (5) doesn't work since phase function $\varphi(\mathbf{r},t)$ is not uniquely defined. Geometry of 2π–phase cuts in phase function $\varphi(\mathbf{r},t)$ can be changed without having any impact on optical field complex amplitude that is proportional to $\exp\left[i\varphi(\mathbf{r},t)\right]$ but at the same time this change affects the piston phase since the aperture averaged value of phase function in (5) depends on 2π–phase cuts geometry. To address this problem, we introduce here a different definition of piston phase that is insensitive to presence of phase singularities. We define piston phase $\overline{\varphi}_1(t)$ as solution of the following equation:

$$\int_{S_a} \sin\left(\varphi(\mathbf{r},t) - \overline{\varphi}_1(t)\right) d^2\mathbf{r} = 0\,, \tag{6}$$

In this definition, one can add 2π value to at any point $\mathbf{r}$ inside receiver aperture without changing piston phase $\overline{\varphi}_1(t)$. The solution of (6) can be represented in the form:

$$\overline{\varphi}_1(t) = \tan^{-1}\left[\frac{\int_{S_a}\sin\left(\varphi(\mathbf{r},t)\right)d^2\mathbf{r}}{\int_{S_a}\cos\left(\varphi(\mathbf{r},t)\right)d^2\mathbf{r}}\right], \tag{7}$$

Note that although the phase defined by (6) is insensitive to 2π phase cuts (jumps), its value still is not uniquely defined because function $\tan^{-1}$ in (7) is a multivalued function with infinite number of separated by π branches. The presence of branch points can result in uncertainty in selection of one or another branch of this function. A special technique based on analysis of phase function and location of phase singularities was applied to minimize impact of 2π phase cuts and branch points on the piston phase computation. The method of piston phase computation based on (7) was compared with the corresponding computations using conventional piston phase function $\varphi(\mathbf{r},t)$. The comparative analysis was performed for D=0.5 m and the outer scale values ranging from L_0=D to L_0 =10 D. As illustrated in Fig. 7, the obtained values of standard deviations for the piston phases $\overline{\varphi}(t)$ and $\overline{\varphi}_1(t)$ coincide with good accuracy which supports legitimacy of the introduced piston phase definition (7).

Consider now results of analysis of piston phase as defined by (7) in deep turbulence conditions characterized by strong scintillations. In the numerical simulations we used three statistically independent extended phase screens. The first phase screen was located in the receiver telescope pupil plane at z=z_1=0 and the second and third phase screens at distances z_2= 0.025 kD^2 and z3= 0.05 kD^2 from the receiver plane. All three phase screens were literary translated to account for wind speed $\mathbf{v}$=(v_x=1.0 m/sec, 0).

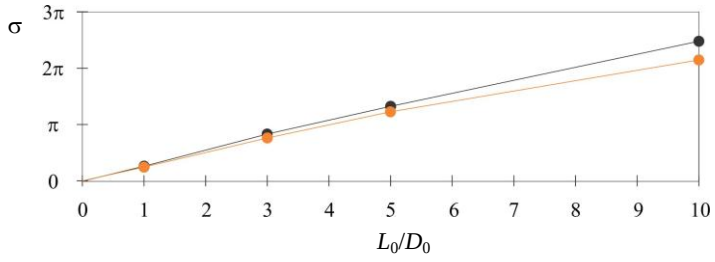

Fig. 7. Dependence of piston phase standard deviation σ on turbulence outer scale L_0 for the case of pupil plane phase screen (Tatarskii power spectrum, C_n^2 = 10^{-15} $m^{-2/3}$ and D_0=0.5 m). The top curve corresponds to the conventional piston phase definition (5) and the bottom line to the piston phase definition (7) which is introduced for piston phase analysis in deep turbulence conditions.

The results of piston phase dynamics over 24 min time interval are presented in Fig. 8 for two different values of the turbulence outer scale.

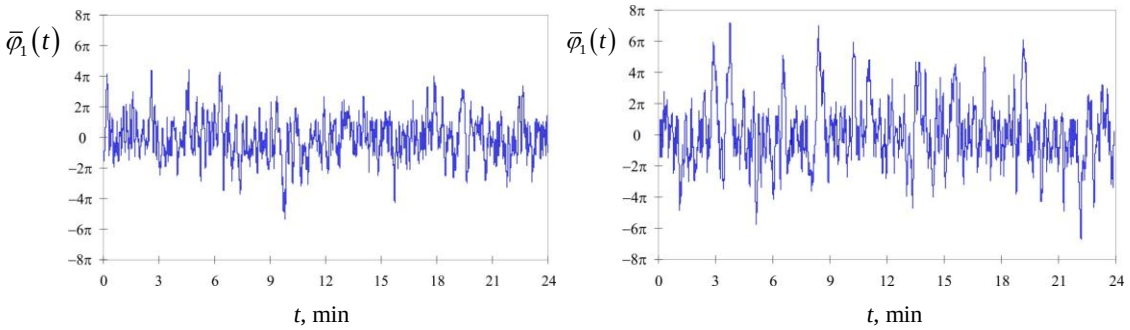

Fig. 8. Temporal evolution of piston phase in deep turbulence conditions that are generated using three distant phase screens for L_0 =5D (left) and L_0 =10D (right) for C_n^2 = 10^{-15} $m^{-2/}3$, and D=0.5 m.

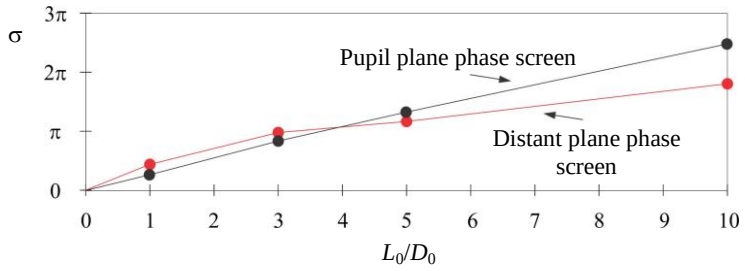

Fig. 9. Piston phase standard deviation σ vs turbulence outer scale L_0 for pupil plane and distant phase screens (C_n^2 = 10^{-15} $m^{-2/}3$ and D_0=0.5 m).

Comparison of piston phase fluctuations for a single phase screen located either at the pupil plane or shifted a distance z_3= 0.05 kD^2 from the receiver pupil (distant phase screen) are presented in Fig. 9, where the standard deviation of the piston phase is shown as a function of the outer scale. The results show that for L_0 < 5D characteristic range of piston phase fluctuations as measured by its standard deviation is nearly identical for both pupil and remotely located phase screens. With increase of the outer scale, the piston phase fluctuations are smaller for the remotely located phase screen (deep turbulence).

4. REFERENCES

[1] C. J. Pellizzari, C. L. Matson, and R. Gudimetla, Inverse synthetic aperture ladar for geosynchronous space objects – signal-to-noise analysis, in Proceedings of the 2011 Advanced Maui Optical and Space Surveillance Technologies Conference (AMOS), (2011).

[2] C. S. Gardner, Effects of random path fluctuations on the accuracy of laser ranging systems, Appl. Opt. **15**, 2539–2545 (1976).

[3] A. M. Vorontsov, P. V. Paramonov, M. T. Valley, and M. A. Vorontsov, Generation of infinitely long phase screens for modeling of optical wave propagation in atmospheric turbulence, Waves in Random and Complex Media **18**, 91–108 (2008).